ISSN 1674-1056
http://cpb.iphy.ac.cn
http://iopscience.iop.org/cpb
中国物理 B
Chinese Physics
中国物理
Chinese Physics B

Enhancement of corona discharge induced wind generation with carbon nanotube and titanium dioxide decoration

Jianchun Ye(叶建春), Jun Li(李俊), Xiaohong Chen(陈晓红), Sumei Huang(黄素梅), Wei Ou-Yang(欧阳威)
Citation: Chin. Phys. B . 2019, 28(9): 095202 . **doi:** 10.1088/1674-1056/28/9/095202
Journal homepage: http://cpb.iphy.ac.cn; http://iopscience.iop.org/cpb

What follows is a list of articles you may be interested in

Electrical and thermal characterization of near-surface electrical discharge plasma actuation driven by radio frequency voltage at low pressure

Zhen Yang(杨臻), Hui-Min Song(宋慧敏), Di Jin(金迪), Min Jia(贾敏), Kang Wang(王康)
Chin. Phys. B . 2018, 27(8): 085205 . **doi:** 10.1088/1674-1056/27/8/085205

Electric ignition energy evaluation and the energy distribution structure of energy released in electrostatic discharge process

Qingming Liu(刘庆明), Jinxiang Huang(黄金香), Huige Shao(邵惠阁), Yunming Zhang(张云明)
Chin. Phys. B . 2017, 26(10): 105202 . **doi:** 10.1088/1674-1056/26/10/105202

Conversion of an atomic to a molecular argon ion and low pressure argon relaxation

M N Stankov, A P Jovanović, V Lj Marković, S N Stamenković
Chin. Phys. B . 2016, 25(1): 015204 . **doi:** 10.1088/1674-1056/25/1/015204

Growth of small diameter multi-walled carbon nanotubes by arc discharge process

K. T. Chaudhary, J. Ali, P. P. Yupapin
Chin. Phys. B . 2014, 23(3): 035203 . **doi:** 10.1088/1674-1056/23/3/035203

Parametric instabilities in single-walled carbon nanotubes

He Cai-Xia, Jian Yue, Qi Xiu-Ying, Xue Ju-Kui
Chin. Phys. B . 2014, 23(2): 025202 . **doi:** 10.1088/1674-1056/23/2/025202

Enhancement of corona discharge induced wind generation with carbon nanotube and titanium dioxide decoration*

Jianchun Ye(叶建春)[1,†], Jun Li(李俊)[2,†], Xiaohong Chen(陈晓红)[1], Sumei Huang(黄素梅)[1], and Wei Ou-Yang(欧阳威)[1,‡]

[1] *Engineering Research Center for Nanophotonics and Advanced Instrument (Ministry of Education), School of Physics and Materials Science, East China Normal University, Shanghai* 200062, *China*

[2] *Department of Electronic Science and Technology, Tongji University, Shanghai* 201804, *China*

(Received 18 April 2019; revised manuscript received 8 July 2019; published online 20 August 2019)

Dip-coated double-wall carbon nanotubes (DWCNTs) and titanium dioxide (TiO_2) sol have been prepared and smeared onto the tip of a conductive iron needle which serves as the corona discharge anode in a needle–cylinder corona system. Compared with the discharge electrode of a CNT-coated needle tip, great advancements have been achieved with the TiO_2/CNT-coated electrode, including higher discharge current, ionic wind velocity, and energy conversion efficiency, together with lower corona onset voltage and power consumption. Several parameters related to the discharge have been phenomenologically and mathematically studied for comparison. Thanks to the morphology reorientation of the CNT layer and the anti-oxidation of TiO_2, better performance of corona discharge induced wind generation of the TiO_2/CNT-coated electrode system has been achieved. This novel decoration may provide better thoughts about the corona discharge application and wind generation.

Keywords: corona discharge induced wind, wind velocity, carbon nanotubes, titanium dioxide

PACS: 52.80.–s, 52.80.Dy, 52.80.Hc, 45.05.+x **DOI:** 10.1088/1674-1056/ab33ed

1. Introduction

Corona discharge-induced wind (CDIW), simply called ionic wind or electric wind, is an airflow induced by corona discharge which is generated from a discharge electrode with a sharp tip (such as a needle, a wire, or a blade) under high voltage. The ionized molecules around the tip accelerate under the high electric field and collide with the surrounding neutral molecules in air, forming an airstream between the electrodes.[1] Compared with a traditional mechanical fan composed of a motor, a speed-regulator, and flabella, CDIW has at least three advantages. (i) It is operated with an extremely low electrical current ($\sim \mu$A), indicating that CDIW is extremely energy-saving and its energy consumption is two orders of magnitude lower than that of the traditional mechanical fans.[2] (ii) CDIW instruments can be fabricated in small size without any moving parts. (iii) CDIW can be easily and quickly generated in atmospheric air, making it suitable for fast-response applications. Hence, CDIW has recently received lots of attention in the fields of heat transfer for cooling devices,[3,4] drying and thawing food,[5,6] and other applications such as electrostatic precipitators,[7] plasma actuating systems,[8] air purification,[9] and electrohydrodynamic thrusters.[10,11] In these applications, the strength of CDIW is a prerequisite and thus strategies to improve CDIW are of particular importance.

Most CDIW instruments consist of a needle-to-collecting electrode system, where the needle with a smaller diameter can generate a large local field intensity when other parameters are fixed. Numerous experimental and analytical investigations have been conducted to study the corona discharge behavior with respect to a series of parameters, such as various electrode configurations,[12,13] wind velocity profile,[14–16] voltage polarity,[16,17] air moisture,[9,14,17] as well as electrode gap.[12,15,18] Meanwhile, nanoscale materials with inherently high aspect ratios, small tip radii, and sharp edges, such as carbon nanotubes (CNTs),[19,20] graphene sheets,[21] ZnO nanowires,[22] and other nanostructures,[23–25] have been investigated for the development of stable atmospheric corona discharges. Among the nano-materials, a thin film of CNTs has been demonstrated as an ideal cathode candidate for electron emission in field emission devices due to the high aspect ratio, outstanding electrical conductivity, excellent chemical stability, and superior mechanical strength and durability.[20,26,27]

However, few studies have previously been carried out to investigate the CDIW of a sharp discharge electrode combined with nanoscale materials from the viewpoint of improving the strength of CDIW. Recently, we invented a simple method to decorate the tip of a discharge needle electrode with a dip-coated CNT thin film and found that the strength of CDIW

*Project supported by the National Natural Science Foundation of China (Grant Nos. 61504042, 61504098, and 61771198), the Natural Science Foundation of Shanghai, China (Grant No. 17ZR1447000), and the Fundamental Research Funds for the Central Universities, China.

†These authors contributed equally to this work.

‡Corresponding author. E-mail: ouyangwei@phy.ecnu.edu.cn

© 2019 Chinese Physical Society and IOP Publishing Ltd

was greatly improved.[2] Meanwhile, our recent studies on the effect of a thin film of titanium dioxide (TiO_2) nanoparticles coated on the CNT cathode of the field emission devices have presented outstanding properties due to the enhanced edge effect arisen from the unique TiO_2/CNT micro films.[28,29] Inspired by the synergistic effect of the TiO_2/CNT composite, in this article, we utilized dip-coated double-wall carbon nanotube (DWCNT) slurry and prepared TiO_2 sol to decorate a conductive iron needle tip as the discharge electrode so as to acquire better efficiency of ionic wind.

2. Experiments

An ordinary iron needle was used as the referential discharge electrode with a diameter of 2.54 mm measured by the thickness gauge instrument. The bare needle was cleaned following a common cleaning process for silicon wafers[30] by acetone, isopropanol, and deionized water sequentially under an ultrasonic environment. For comparison, two kinds of other discharge electrodes were made based on the bare electrode. One was prepared by coating a thin layer of CNTs onto the tip of the needle, and the other was fabricated by further coating a thin layer of TiO_2 on the surface of the CNT thin film. For preparation of the CNT-coated electrode, DWCNTs (purity $>$ 90%, diameter $<$ 5 nm, length 5–15 μm, Shenzhen Nanotech Port Co., Ltd, China) were used and the details of the coating process were described in our previous article.[2] For the fabrication of the TiO_2/CNT-coated electrode, TiO_2 sol was first synthesized through the hydrolysis and condensation of tetrabutyl titanate ($Ti(OC_4H_9)_4$) following our previous article and then dip-coated onto the CNT-coated discharge electrode following by a drying process of 200 °C for 10 min and a subsequent annealing process of 350 °C for 30 min.[28]

The experimental appliance is sketched in Fig. 1. The iron needle served as the discharge anode while the thin copper cylinder with an inner diameter of 19.46 mm was the cathode. The needle electrode was mounted at the axis of the cylinder electrode to achieve optimum performance and the distance between the electrodes (also called the electrode separation or electrode gap) was fixed at 5.5 mm. The power was provided by a high-voltage direct current power supply which could generate and regulate the output voltage from 0 to 30 kV with the resolution of 0.01 kV. The electric current was measured using a multimeter with the accuracy of 0.1 μA. The needle was connected to the negative pole of the high voltage power supply while the copper cylinder was safely grounded. The whole corona wind generating device was positioned in a polymethyl methacrylate (PMMA) tube with the inner diameter of 19.50 mm. The hot wire anemometer (AM-4204HA, Lutro Electronic Enterprise Co. Ltd, China) with the range of 0–20 $m{\cdot}s^{-1}$ and resolution of 0.1 $m{\cdot}s^{-1}$ was attached to the outlet of our apparatus to examine the practical velocity of the ionic wind. The corona discharge test was conducted at ambient air. Note that the measured wind velocity at the outlet is larger than the average speed of the airflow in the PMMA tube and it can be amplified by assembling a number of discharge electrodes in parallel.[1]

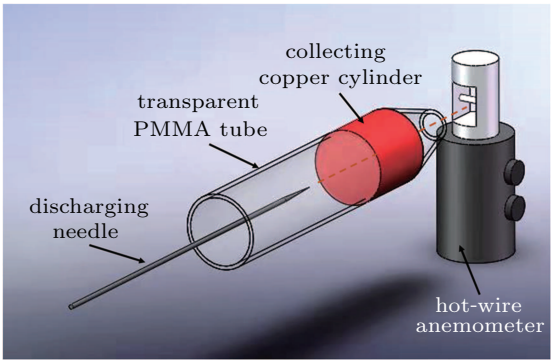


Fig. 1. Sketch of experimental appliance for CDIW generation. The diameter of the copper cylinder electrode is 19.46 mm, the inner diameter of the PMMA tube is 19.50 mm, and the distance between the electrodes is 5.5 mm.

3. Results and discussion

The relationship between the corona current (I) and the applied voltage (V) for various experimental electrodes is plotted in Fig. 2. All three curves in Fig. 2(a) tend to become steeper as the voltage increases. This means that the electrical resistance of the gas channel between the two electrodes tends to lessen when a higher voltage is applied especially as the discharge devices are close to spark over. In addition, once the applied voltage reaches the corona onset voltage (V_0, defined at the corona current of 0.1 μA), the electrical current flows from the needle to the grounded electrode because of the ionization of air near the discharge needle tips. The onset voltage is the smallest for the TiO_2/CNT-coated electrode (5.9 kV) whilst the largest for the bare electrode (6.9 kV). As a result, when an identical corona voltage is applied, the TiO_2/CNT-coated device can acquire the highest discharge current. The diminutive discharge onset voltage is necessary and desirable for industrial applications of CDIW devices as low V_0 probably diminishes the power consumption thus increases the energy conversion efficiency.[13] The helpful ways of minimizing V_0 can be adopted by reducing the discharge size as well as the inter-electrode spacing. However, the lowered electrode separation may cause reduced ionic wind velocity while the identical input power is exerted.[31,32] As a consequence, external decoration onto the tips/edges of the discharge electrodes is of great significance to obtain minor onset voltage. Since the air between the two electrodes would almost not be heated during the discharge process, the temperature of air can be basically unchanged during the discharge process. As a result, the descended V_0 for the TiO_2/CNT-coated device is unrelated to the temperature.[33]

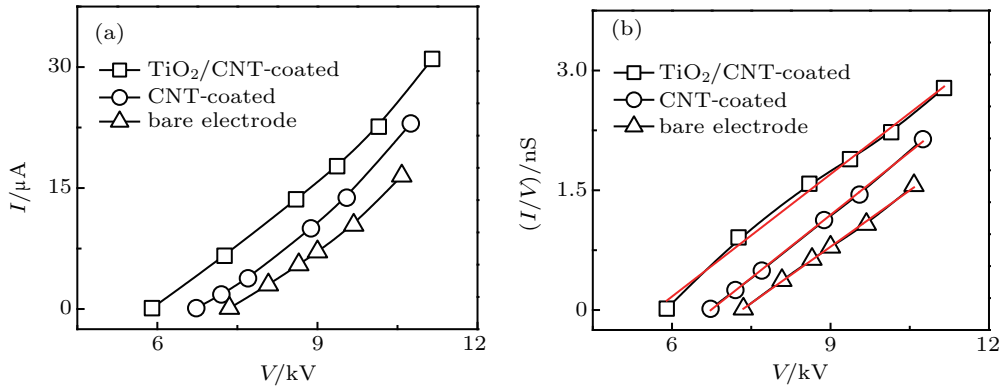


Fig. 2. Current–voltage characteristics of the as-prepared electrodes: (a) *I*–*V* curves, (b) I/V–V curves (the red lines are linear fittings for the experimental data).

Table 1. Calculated parameters of various electrodes.

Electrode	B /10^{-12} A·V^{-2}	μ /cm^2·V^{-1}·s^{-1}	ν_m /10^{15} s^{-1}	g_3 /10^{-3} m·V^{-1}·s^{-1}
TiO_2/CNT-coated	0.51	0.46	3.86	0.24
CNT-coated	0.53	0.47	3.72	0.21
Bare electrode	0.47	0.42	4.19	0.31

Figure 2(b) depicts the ordinary conductivity with respect to the applied voltage (I/V–V curves) of the as-prepared devices. The almost linear curves manifest that the discharge performance follows the Townsend's relation for all of our devices[34]

$$I = BV(V - V_0), \tag{1}$$

where I is the corona discharge current (in A), V is the applied voltage (in V), V_0 is the corona onset voltage (in V), and B is the dimensional constant depending on the mobility of charge carriers in the drift region and the geometrical factors of the devices such as the inter-electrode distance, the radius of the needle electrode, etc. The fitting slopes B in Fig. 2(b) are listed in Table 1. Herein, we have recognized that there is another definition form of conductivity, i.e., the differential conductivity, which has been intensively studied in graphene related electronic devices recently.[35–37] Therefore, we plot the differential conductivity with respect to the applied voltage for guiding the eyes (see Fig. S1 in the supplementary material) and the results confirm that the discharge process follows the Townsend's relation.

The slope B in Fig. 2(b) can be elaborately defined to search the ionic mobility (μ) of corona discharge[2]

$$I = \frac{8\pi\varepsilon\mu V(V - V_0)}{R\ln(R/r)}, \tag{2}$$

where ε is the absolute dielectric permittivity of the gas medium in F·m^{-1}, which approximates to the dielectric constant ε_0 of vacuum (8.854×10^{-12} F·m^{-1}), μ is the carrier mobility of the ionized gas in m^2·V^{-1}·s^{-1}, and r and R are the radii of the needle and cylindrical electrodes in m, respectively. The calculated ionic mobilities in our experimental devices correspond to the ionic mobility of common discharged air,[1] and are comparable with the state-of-the-art organic and inorganic semiconductors.[38,39] What seems interesting is that the CNT-coated electrode manifests the highest ionic mobility of 0.47 cm^2·V^{-1}·s^{-1} while the bare electrode reveals the minimum ionic mobility of only 0.42 cm^2·V^{-1}·s^{-1}. Therefore, DWCNTs and the further coated TiO_2 thin layer do have an effect on accelerating the migration of ions.

In the gas phase, the ionic mobility can be defined as

$$\mu = \frac{e}{m_e \nu_m}, \tag{3}$$

where e is the elementary charge in C, m_e is the electron mass in kg, and ν_m is the collision frequency for electron momentum transfer in s^{-1}. From Eq. (3), ν_m can be obtained for various experimental electrodes and listed in Table 1 for comparison. Noted that the calculated collision frequency is three orders of magnitude higher than the reported results because the international system of units is used in this study.[2,40]

The electric wind velocity (v) as a function of the applied voltage (V) is shown in Fig. 3. The wind velocity increases more sharply in the lower voltage region (below 8 kV) and then ascends more slowly in the higher voltage region. The TiO_2/CNT-coated electrode can achieve a larger velocity than the other two counterparts when the identical voltage is applied and manifest the maximal peak velocity of 1.8 m·s^{-1}. The connection of the current with the ionic wind velocity is given by[34]

$$v = \frac{g_1}{\sqrt{\rho_g \mu}}\sqrt{I}, \tag{4}$$

where g_1 is an appropriate function of the geometry and inversely proportional to the square root of the aerodynamic loss coefficient K, and ρ_g is the density of air (in g·cm^{-3}). The Reynolds number (R_e) for Newtonian fluid (e.g., air flow in this work) flowing in a tube can be defined as

$$R_e = \frac{\rho_g v D}{\eta}, \tag{5}$$

where D is the diameter of the tube in m and η is the dynamic viscosity of the ionic air in Pa·s. As we know, the laminar flow is generally determined with $R_e < 2000$ while the turbulent flow is defined when $R_e > 4000$ for the fluid in a

tube. The Reynolds number between 2000 and 4000 is the transition flow from laminar to turbulent flow.[41] Supposing the ionic wind velocity is 1.8 m·s^{-1} (which is comparable to our maximal wind velocity available), the simply calculated Reynolds number is 2358. Considering the wind velocity in the tube is much smaller than that recorded at the outlet, the real Reynolds number shall be much lower than the critical value of 2000 and thus the air flow in the CDIW tube is a kind of laminar flow. Furthermore, the air velocity can be even smaller at the lower voltage region which symbolizes that laminar flow plays a leading role for CDIW in a tube. Note that the larger Reynolds number obtained from the TiO_2/CNT-coated electrode contributes to the lower aerodynamic loss coefficient K.[2]

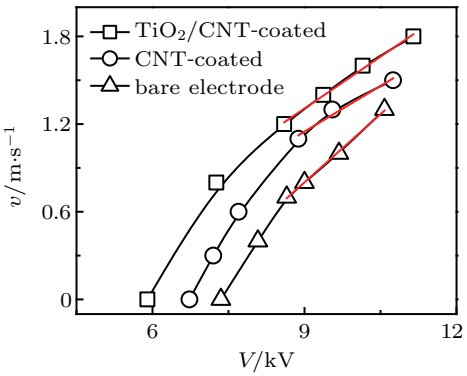


Fig. 3. Ionic wind velocity v as a function of discharge voltage V for various electrodes (the red lines are linear fittings for the data at high voltage regions).

Using the following two parameters:

$$g_2 = 8\pi\varepsilon/[\rho_g R \ln(R/r)], \tag{6}$$

$$g_3 = g_1 g_2^{1/2}, \tag{7}$$

and correlating Eq. (2) with Eq. (4), we can obtain

$$v = g_3 [V(V - V_0)]^{1/2}, \tag{8}$$

$$v \approx g_3 V, \quad (V \gg V_0). \tag{9}$$

The v–V curves (as shown in Fig. 3) in the high-voltage domain are approximately linear, which accord to the deduced equations above. The fitting slopes, i.e., the slope g_3 in Eq. (9), of our experimental data for the three electrodes are listed in Table 1 as well and the slope g_3 reduces successively for bare, TiO_2/CNT-coated, and CNT-coated electrodes. There are several merits of CNTs such as high electrical conductance, glorious mechanical properties, as well as unique aspect ratios.[27,42–44] It is convenient to form an extremely high local electric field at the vicinity of the tips. The annealing procedure of the TiO_2 layer can produce plenty of teeny modules on the TiO_2/CNT nano-composite thin membrane. CNTs become more prominent and upright under the impact of these modules, leading to the diminishment of the shielding effect as well as the enhancement of the fringe effect.[28] The local electric field strength adjacent to the tip of the TiO_2/CNT-coated discharge electrode would be even huge contributing to the declined onset voltage and incremental wind velocity. Moreover, the tendency of the v–V curves for our electrodes approaches to the computational fluid dynamics results and thus the energy loss is less.[45]

The power consumption as well as the operation efficiency may be of great concern for electrical devices. It is urgent to search brilliant low-powered CDIW cooling apparatus in order to replace conditional cooling fans. The kinetic output power P_0 (in W) as a function of CDIW velocity v is given as[34]

$$P_0 = \frac{1}{2}\rho_g S v^3, \tag{10}$$

where S is the cross-sectional area of the PMMA tube at the outlet (in m^2) of the PMMA tube for our experimental setup. The calculated kinetic output power P_0 using the above equation depending on CDIW velocity v is given in Fig. 4(a). Among our fabricated electrodes, the TiO_2/CNT-coated one gives the optimal output power. The electrokinetic energy conversion efficiency (ECE) η_e is defined as[34]

$$\eta_e = \frac{P_0}{P_i} = \frac{P_0}{VI}, \tag{11}$$

where P_i is the input power in W.

The electrokinetic energy conversion efficiency is commonly knockdown for CDIW devices ($\eta_e < 1\%$), impeding the practical application severely.[31,34,46] However, there is scarcely any effective techniques to improve ECE. Higher ECE can be achieved by decreasing the input power (i.e., the power dissipation) and/or increasing the output power. Therefore, the way to attain high output work is quite imperative and the novel electrode decoration in this article can surprisingly give rise to better ECE. As seen in Fig. 4(b), the TiO_2/CNT-coated electrode exhibits the best ECE. That is because the ionic wind velocity v of the TiO_2/CNT-coated electrode is the largest among the three electrodes when the applied voltage is the same (manifested in Fig. 3). Consequently, the corona discharge performance of the TiO_2/CNT-coated electrode is optimal, which makes it a promising candidate for CDIW generators. The decline of η_e at the applied voltage over 10 kV is probably caused by the sharply decreased electrical resistance of the air channel between the two electrodes as the discharge apparatus nearly breaks down which is in accordance with the discussion of Fig. 2(a).

Furthermore, DWCNTs have poor adhesion to the conductive substrate, causing an unwanted contact resistance, which in turn creates the heating effect.[47–49] The poor adhesion may be a barrier for electrical carriers to transport during the discharge process. The created heating effect would ascend the electrical resistance of the discharge needle and

then the corona current falls off. DWCNTs can be easily degraded as a result of oxidation and heating effect on the surface of the electric conductor.[43] The degradation of DWCNTs might be more severe when corona discharge happens because plasma, free radical, as well as ozone can easily destroy DWCNTs at the surface of the discharge electrode. TiO_2 is a natural dioxide to wrap the in-layer DWCNTs for avoiding degradation.[28,43] It can overcome the oxidation of DWCNTs efficiently especially during the discharge procedure. DWCNTs and TiO_2 composites have shown enhanced thermal conductivity.[50] It appears that the TiO_2/CNT-coated electrode exhibits better performance as the heating effect might be perfectly resolved. The highest output power as well as energy conversion efficiency of the TiO_2/CNT-coated electrode could be verified and explained excellently. Hence, the DWCNTs and TiO_2 nano-composites seem to be an awesome combination to realize satisfactory corona discharge effectiveness for CDIW electrical devices.

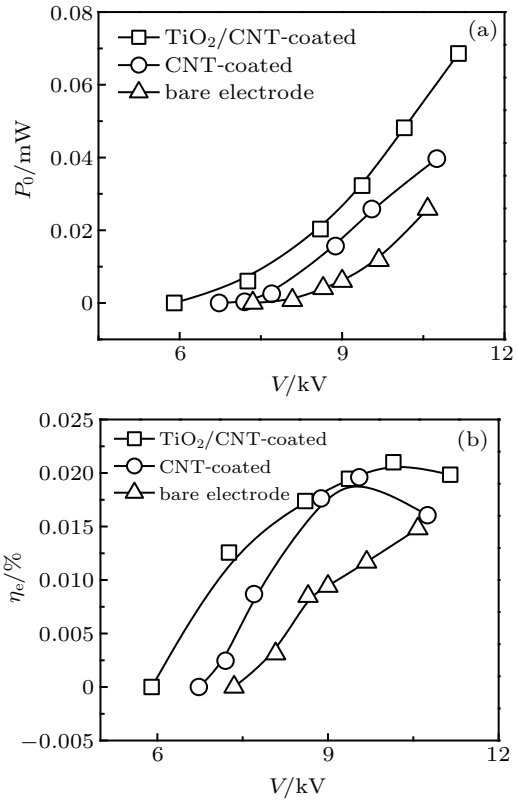


Fig. 4. (a) Corona discharge output power (P_0) and (b) efficiency (η_e) as a function of voltage (V) for various electrodes.

4. Conclusion

Dip-coated DWCNTs combined with TiO_2 sol have been decorated on the tip of corona needles and have presented scores of merits including lower corona onset voltage, higher CDIW velocity, larger output power, and better energy conversion efficiency. The corona discharge characteristics adhere to the Townsend's discharge rules as well as the equations presented in the previous publications. In addition to the phenomenological explanation of our experimental data, a series of parameters such as ionic mobility, Reynolds number, and so on for various experimental electrodes are calculated, linearly fitted, and discussed for comparison. The TiO_2/CNT-coated device shows the optimal capability for CDIW appliance. The superiority of the coated DWCNTs and TiO_2 layers is mainly ascribed to the natural oxidation and protection of TiO_2 as well as the particular aspect ratios of DWCNTs. TiO_2 and DWCNTs nano-composites may exhibit better electrical and thermal conductivity, less heating effect, and descended contact resistance. In conclusion, DWCNTs with unique high aspect ratios and electrical conductivity companied with natural anti-oxidation of TiO_2 contribute to marvelous CDIW manifestation of our apparatus. It is worth drawing on the experience of our neoteric decoration techniques and inspiration for future corona discharge as well as aerodynamics researches.

Acknowledgment

The authors thank Miss. Xiao Meng for her help in figure drawing.

References

[1] Robinson M 1962 *Am. J. Phys.* **30** 366
[2] Wu Y, Li J, Ye J, Chen X, Li H, Huang S, Zhao R and Ou-Yang W 2017 *J. Phys. D: Appl. Phys.* **50** 395304
[3] Chen I Y, Guo M Z, Yang K S and Wang C C 2013 *Int. J. Heat Mass Transf.* **57** 285
[4] Kim B, Lee S, Lee Y and Kang K H 2012 *J. Electrostat.* **70** 438
[5] He X, Jia G, Tatsumi E and Liu H 2016 *Innov. Food Sci. Emerg.* **34** 135
[6] Choi S, Puligundla P and Mok C 2017 *LWT - Food Sci. Tech.* **75** 323
[7] Wen T Y, Wang H C, Krichtafovitch I and Marnishev A V 2015 *J. Electrostat.* **73** 117
[8] Yang Z, Song H M, Jin D, Jia M and Wang K 2018 *Chin. Phys. B* **27** 085205
[9] Timmermann E, Prehn F, Schmidt M, Höft H, Brandenburg R and Kettlitz M 2018 *J. Phys. D: Appl. Phys.* **51** 164003
[10] Drew D S and Pister K S J 2017 *Micromachines* **8** 141
[11] Audier P, Fénot M, Bénard N and Moreau E 2016 *Appl. Phys. Lett.* **108** 084103
[12] Azooz A A and Talal S K 2011 *Chin. Phys. Lett.* **28** 115202
[13] Eifert A, Baier T and Hardt S 2013 *Appl. Phys. Lett.* **103** 023114
[14] Lee J R and Lau E V 2017 *Appl. Therm. Eng.* **114** 554
[15] Zhang Y, Liu L, Chen Y and Ouyang J 2015 *J. Electrostat.* **74** 15
[16] Moreau E, Audier P and Benard N 2018 *J. Electrostat.* **93** 85
[17] Chen S, van den Berg R G W and Nijdam S 2018 *Plasma Sources Sci. T.* **27** 055021
[18] Li H, Jiang L, Guo C, Zhu J, Jiang Y, Xiao W, Fang C and Chen Z 2017 *J. Electrostat.* **86** 59
[19] Nahan K S, Alvarez N, Shanov V and Vonderheide A 2017 *J. Am. Soc. Mass Spectrom.* **28** 2408
[20] Bo Z, Yu K, Lu G, Mao S, Chen J and Fan F 2010 *Environ. Sci. Tech.* **44** 6337
[21] Bo Z, Yu K, Lu G, Cui S, Mao S and Chen J 2011 *Energy Environ. Sci.* **4** 2525
[22] Yang W, Zhu R and Zong X 2016 *Nanoscale Res. Lett.* **11** 1
[23] Lv W Q, Wang L P, Cao Y Z, Gu Z W, Wang X F, Yan Y D and Yu F L 2016 *Chin. Phys. Lett.* **33** 095201
[24] Ye S, Liang J, Song X, Luo S and Liang J 2016 *Biosyst. Eng.* **150** 123
[25] Sadeghian R B and Islam M S 2011 *Nat. Mater.* **10** 135
[26] Xu J, Xu P, Guo P, Ou-Yang W, Chen Y, Feng T, Piao X, Wang M and Sun S 2015 *RSC Adv.* **5** 21755
[27] Song Y, Li J and Ou-Yang W 2019 *IEEE Trans. Electron. Dev.* **66** 716

[28] Xu J, Xu P, Ou-Yang W, Chen X, Guo P, Li J, Piao X, Wang M and Sun Z 2015 *Appl. Phys. Lett.* **106** 073501
[29] Wu Y, Li J, Ye J, Song Y, Chen X, Huang S, Sun Z and Ou-Yang W 2017 *J. Alloy. Compd.* **726** 675
[30] Ou-Yang W, Weis M, Taguchi D, Chen X Y, Manaka T and Iwamoto M 2010 *J. Appl. Phys.* **107** 124506
[31] Dau V T, Dinh T X, Bui T T, Tran C D, Phan H T and Terebessy T 2016 *Exp. Therm. Fluid Sci.* **79** 52
[32] Dau V T, Tran C D, Dinh T X, Dang L B, Terebessy T and Bui T T 2018 *IEEE Trans. Dielectr. Electr. Insul.* **25** 900
[33] Gradov O V and Gradova M A 2016 *Surf. Eng. Appl. Electrochem.* **52** 117
[34] Robinson M 1961 *Trans. Am. Inst. Elect. Eng. Part. I: Commun. Electron.* **80** 143
[35] Bandurin D A, Torre I, Kumar R K, Shalom M B, Tomadin A, Principi A, Auton G H, Khestanova E, Novoselov K S, Grigorieva I V, Ponomarenko L A, Geim A K and Polini M 2016 *Science* **351** 1055
[36] Liu N, Liu J B and Yao K L 2017 *AIP Adv.* **7** 125117
[37] Rathi S, Lee I, Kang M, Lim D, Lee Y, Yamacli S, Joh H, Kim S, Kim S, Yun S J, Choi S and Kim G 2018 *Sci. Rep.* **8** 7144
[38] Ou-Yang W, Mitoma N, Kizu T, Gao X, Lin M F, Nabatame T and Tsukagoshi K 2014 *Appl. Phys. Lett.* **105** 163503
[39] Nakayama K, Ou-Yang W, Uno M, Osaka I, Takimiya K and Takeya J 2013 *Org. Electron.* **14** 2908
[40] Ladouceur H D, Baronavski A P, Lohrmann D, Grounds P W and Girardi P G 2001 *Opt. Commun.* **189** 107
[41] Housley D, Huddle T, Lester E and Poliakoff M 2016 *Chem. Eng. J.* **287** 350
[42] Zhang J, Deng Y and Hao T T 2018 *Chin. Phys. B* **27** 128101
[43] Zhu W D, Wang C W, Chen J B, Li D S, Zhou F and Zhang H L 2012 *Nanotech.* **23** 455204
[44] Chen X, Jiang T, Sun Z and Ou-Yang W 2015 *Appl. Phys. Lett.* **107** 114103
[45] Shin D H, Baek S H and Ko H S 2016 *Int. J. Heat Mass Transf.* **93** 516
[46] Zhou D, Tang J, Kang P, Wei L and Zhang C 2018 *J. Electrostat.* **96** 99
[47] Alivov Y, Klopfer M and Molloi S 2010 *Appl. Phys. Lett.* **96** 243502
[48] Zhang G and Huang S Y 2013 *Physics* **42** 100
[49] Zhou K K, Xu N and Xie G F 2018 *Chin. Phys. B* **27** 026501
[50] Khosravifard E, Salavati-Niasari M, Dadkhah M and Sodeifian G 2012 *J. Nanostruct.* **2** 191